THE ASTROPHYSICAL JOURNAL, 390:96–104, 1992 May 1

PROPAGATION OF COSMIC-RAY NUCLEI IN A DIFFUSING GALAXY WITH CONVECTIVE HALO AND THIN MATTER DISK

W. R. WEBBER,[1] M. A. LEE,[2] AND M. GUPTA[1]

Received 1991 April 18; accepted 1991 November 7

ABSTRACT

We have utilized a diffusion model for cosmic-ray propagation in the galaxy that includes the effects of convection in the halo. This model has several novel features. The matter is assumed to be distributed within an infinitely thin disk within which the sources are also found. Calculations are made for 13 primary and secondary nuclei with rigidities between 1 and 10^3GV. These calculations are made using interaction loss rates, secondary production rates, and radioactive decay, based on recent new cross section measurements. We find that in order to fit the rather weak radial dependence of cosmic-ray protons derived from gamma-ray data, the radial profile of the cosmic-ray sources must also have a weak radial dependence. Large halos that could redistribute the cosmic rays into flatter radial profiles are ruled out from a study of cosmic-ray primary to primary, secondary to primary, and radioactive decay isotope abundance ratios. The most sensitive of these ratios using current data are the secondary to primary ratios, B/C and $Z = 21$–23/Fe. These ratios set limits on the halo thickness of less than 4 kpc and a galactic wind convection velocity less than 20 km s^{-1} within this distance from the plane. These limits are interrelated, however, so that as $L \rightarrow 4$ kpc, $V_c \rightarrow 0$. The data on radioactive secondaries set similar limits although because of the accuracy of the data and the lack of high-energy measurements these limits are not as stringent as they could be. These results suggest that convection perpendicular to the disk of our galaxy may not be important even at rigidities less than a few GV. These limits on halo thicknesses are consistent with what can be determined for the distribution of cosmic-ray electrons in the halo based on the distribution of radio synchrotron emission in our galaxy and other galaxies.

Subject headings: convection — cosmic rays — galaxies: structure

1. INTRODUCTION

The distribution of cosmic-ray nuclei in the galaxy is determined by several factors such as the distribution of cosmic-ray sources, the characteristics of the galactic halo, the magnitude of the diffusion coefficient, and energy loss processes. Clues as to the nature and distribution of the cosmic-ray sources as well as their propagation come from studies of the distribution of radio and gamma-ray emission in the galaxy. The most recent of these studies seems to show that the cosmic-ray proton distribution in the galactic disk, as derived from the gamma-ray emissivity, falls off slowly with radius with an effective scale length r_0 of greater than 20 kpc (Bloemen 1989).

We have developed a diffusion model which incorporates a thin matter disk to study the effect of the cosmic-ray source distribution on the radial distribution of cosmic rays in the galaxy (Gupta, Lee, & Webber 1990). This model has been extended in this paper to determine the distribution of primaries, secondaries, and radioactive secondaries as a function of rigidity (energy). The specific interaction loss and secondary production terms for each nucleus are included in the calculation. The effects of a galactic wind perpendicular to the disk are also considered. In the sense of the above new features these calculations represent an extension of several earlier calculations using diffusion models with halos (e.g., Owens & Jokipii 1977; Ginsburg, Khazan, & Ptuskin 1980; Kota & Owens 1980; Freedman et al. 1980; Lerche & Schlickeiser 1982). Our calculations are compared with gamma-ray observations and also with cosmic-ray data on the energy spectra of the different primary species and secondary/primary charge ratios such as B/C and $Z = 21$–23/Fe. Predictions are also made for the radioactive species ^{10}Be and ^{26}Al.

2. THE MODEL AND THE INPUT PARAMETERS TO THE CALCULATIONS

For the galaxy we have assumed a cylindrical diffusing halo with $0 < r < R = 20$ kpc and $-L < z < L$, where L is variable. Free escape is assumed at the boundaries so that $N(|z| = L) = N(r = R) = 0$. The diffusion coefficient K is assumed to be independent of spatial coordinates throughout the diffusing volume but dependent on rigidity. A novel feature of our model is that the matter is assumed to be distributed uniformly within a very thin matter disk of half-height $h = 100$ pc, much smaller than L. For the purposes of this calculation the disk is assumed to be infinitely thin. Various radial distributions of primary sources are assumed; these are also confined to the thin matter disk. A galactic wind of velocity V_c is assumed to convect particles perpendicular to the disk. Both interaction loss and secondary production are assumed to occur in the thin disk only. Radioactive decay occurs throughout the diffusing volume.

The transport equation for a primary species is then

$$\frac{\partial N}{\partial t} = 0 = -\frac{\partial}{\partial z}(V \cdot N) + K\left[\frac{\partial^2 N}{\partial z^2} + \frac{1}{r}\frac{\partial}{\partial r}\left(r\frac{\partial N}{\partial r}\right)\right] - 2h\Gamma_p \delta(z) N + 2h\delta(z) Q(r) ,$$

where $N(r, z)$ is the number density of the primaries, and Γ_p is the interaction rate of the particular primary species in the disk $= nv\sigma_p$, where n is the density in the disk $= 1$ cm^{-3} and σ_p is the interaction cross section.

[1] Particle Astrophysics Lab and Astronomy Department, New Mexico State University, Las Cruces, NM 88003.
[2] Space Science Center, University of New Hampshire, Durham, NH 03824.

For stable and unstable secondaries we have

$$\frac{\partial M}{\partial t} = 0 = -\frac{\partial}{\partial z}(V \cdot M) + K\left[\frac{\partial^2 M}{\partial z^2} + \frac{1}{r}\frac{\partial}{\partial r}\left(r\frac{\partial M}{\partial r}\right)\right] - 2h\Gamma_s \delta(z)M - \Gamma_r M + 2h\Gamma_{ps}\delta(z)N ,$$

where $M(r, z)$ is the number density of the particular secondary species, Γ_s is the interaction rate of the particular secondary species in the disk, Γ_r is the radioactive decay loss rate and Γ_{ps} is the total rate of production of the secondary species in the disk.

Note that rigorously $N(r, z)$ is the total number density of particles integrated over energy under the assumption that the parameters K and the spallation rates are independent of energy. We take $N(r, z, P)$ calculated with these parameters and Q dependent on energy to be representative of the differential density even though this procedure neglects the adiabatic deceleration which occurs at $z = 0$ if $V_c = 0$. For $V_c = 0$, $N(r, z, P)$ obtained as prescribed is rigorously the differential density.

The values for σ_p, σ_s, and σ_{ps} used in the calculations are listed in Table 1 for energies greater than 1.5 GeV per nucleon. A total of 13 separate species are considered; H, He, Be, ^{10}Be, B, C, N, O, Al, ^{26}Al, Si, $Z = 21$–23, and Fe.

For the secondary production terms, Γ_{ps}, we have evaluated the total production into a particular secondary species from all heavier primaries, weighted by the primary abundance, using the newly measured and predicted cross sections of Webber, Kish, & Schrier (1990 a, b, c). In evaluating the Γ_p, Γ_s, and Γ_{ps} terms for particles of different energy (rigidity), we have allowed the particle velocity to change and have used the measured or predicted variation of the cross sections with energy. This calculation therefore approximates quite closely the usual leaky box model (LBM) calculations (Soutoul et al. 1985) except for the effects of ionization energy loss which are not explicitly included in the model and are treated separately.

The solutions may be obtained separately for primaries and secondaries using eigenfunction expansions in r. For primaries, we have at $z = 0$:

$$N = \sum_i q_i A_i^{-1} J_0(\xi_i \rho)$$

where

$$\rho = r/R$$

TABLE 1

CROSS SECTIONS USED IN CALCULATIONS
($E > 1.5$ GeV per nucleon)
(σ in mb)

Charge	σ_p	σ_s	σ_{ps}
H	44	...	...
He	105	...	...
Be	...	190	48
^{10}Be	...	212	8
B	...	232	167
C	250	...	...
N	...	275	138
O	308	...	...
Al	...	450	162
^{26}Al	...	434	45
Si	465	...	...
$Z = 21$–23	...	696	216
Fe	760	...	...

and

$$A_i = V_c + 2h\Gamma_p + KS_i \coth(\tfrac{1}{2}LS_i)$$

and

$$q_i = Q(P)(\pi R^2)^{-1}[J_1(\xi_i)]^{-2}\left(\int_0^1 d\rho\, \rho^{\alpha+1} e^{-\beta\rho}\right)^{-1} \times \int_0^1 d\rho\, \rho^{\alpha+1} e^{-\beta\rho} J_0(\xi_j \rho) ,$$

where

$$S_i = (V_c^2 K^{-2} + 4\xi_i^2 R^{-2})^{1/2}$$

and where j_0 and J_1 are Bessel functions and ξ_i is the ith zero of J_0. $Q(P)$ is the total differential production of cosmic rays in the galaxy in units of (s-momentum)$^{-1}$.

For secondaries the solution is

$$M = 2h\Gamma_{ps} \sum_i q_i A_i^{-1} B_i^{-1} J_0(\xi_i \rho)$$

where

$$B_i = V_c + 2h\Gamma_s + KS_i' \coth(\tfrac{1}{2}LS_i')$$

and

$$S_i' = (V_c^2 K^{-2} + 4\xi_i^2 R^{-2} + 4\Gamma_r K^{-1})^{1/2} .$$

3. THE CALCULATIONS

3.1. *The Radial Distribution of Protons*

We first determine the radial distribution for protons normalized to 1 at a radius of 10 kpc. For the distribution of primary sources we consider three examples: (1) a flat distribution, $Q(\rho) = Q_0$ (where $\rho = r/R$), (2) a supernova distribution, $Q(\rho) = Q_0 \rho^{1.20} \exp^{-6.44\rho}$ originally used by Stecker & Jones (1977) and (3) modified supernova distribution $Q(\rho) = Q_0 \rho^{0.6} \exp^{-3.0\rho}$, a flatter distribution consistent with the current data on the radial distribution of supernova remnants and pulsars (Lyne, Manchester, & Taylor 1985). We also consider halos of thicknesses between 2 and 16 kpc and vary the diffusion coefficient from 0.3 to 3×10^{28} cm^2 s^{-1}, appropriate for a few GeV protons.

Various combinations of halo thickness and diffusion coefficient will modify the proton radial distribution; however, an important conclusion from these calculations is that the cosmic-ray radial distribution is not a strong function of the size of the halo, for a fixed value of K. For small values of L/R, $N(\rho)$ approaches the source distribution $Q(\rho)$. For larger values of L/R, $N(\rho)$ becomes flatter but is still dominated by the source distribution. This behavior is illustrated in Figure 1 for the supernova distribution used by Stecker & Jones (1977). Here it is seen that for a constant K, even for very thick halos, this supernova radial distribution will not lead to cosmic-ray distributions that are a good match to the cosmic-ray radial distributions derived from the observed gamma-ray emissivity. This conclusion and our calculations in this regard are consistent with the results of Dogiel & Uryson (1988) and Bloemen & Dogiel (1992). These authors need very large halos ($L/R > 0.75$) as well as large diffusion coefficients to approach but not match the derived cosmic-ray radial distribution. This means that to fit the derived cosmic-ray radial distribution it is necessary to assume source distributions that are a weaker function of radius, close in fact to the actually derived cosmic-ray radial distribution. An example of such a radial source distribution,

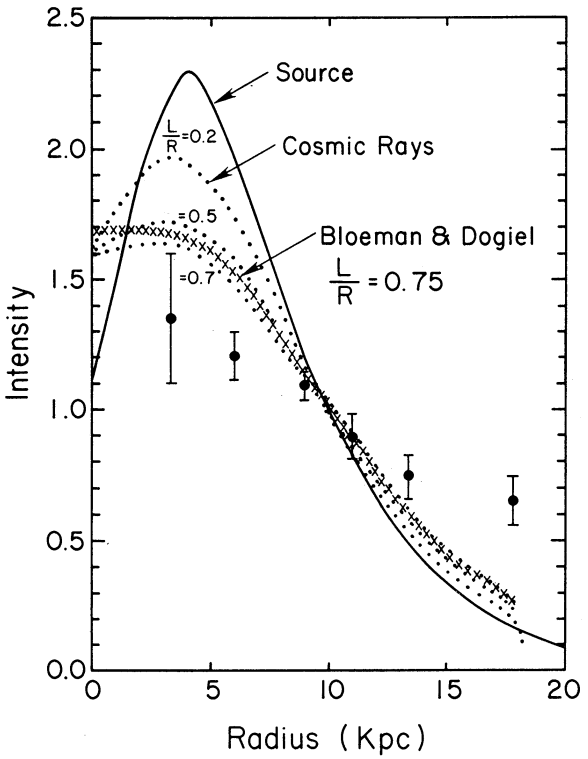

FIG. 1.—Calculated cosmic-ray radial distribution for different halo sizes, K fixed. Source distribution from Stecker & Jones (1977). Cosmic-ray nuclei distribution from Bloemen (1989).

consistent with our current understanding of the radial supernova or pulsar distributions (Lyne et al. 1985; Kassim 1989), is shown in Figure 2. In this example, halos in the thickness range 2–4 kpc are considered. This combination gives a good fit to the radial cosmic-ray proton distribution derived from the gamma-ray data. The calculations to be described next show that, with and without a convective wind perpendicular to the galactic disk, most of the observable quantities related to cosmic rays including (1) the primary energy spectra, (2) the secondary to primary ratios such as B/C and $(Z = 21–23)$/Fe, and (3) the radioactive secondary ratios such as ^{10}Be/Be and ^{26}Al/Al are all consistent with effective halo thicknesses less than 4 kpc.

3.2. *Spectra and Ratios of Individual Nuclei*

For the calculations involving the species listed in Table 1 we take the convective velocity perpendicular to the disk to range from 0 to 80 km s^{-1}. As we noted earlier, interaction loss and secondary production are included for each species according to the values in Table 1. Solutions are obtained for diffusion coefficients ranging from 3×10^{27} to 10^{30} cm^2 s^{-1} corresponding to particle rigidities from ~ 1 to 10^3 GV and the production and loss terms are varied for each species appropriate to the particular rigidity. In this way we can reconstruct the rigidity spectra for all species, assuming a source spectrum of index γ_s. For these calculations the halo size is varied from 1 to 16 kpc.

In these calculations, to gain a perspective, we first consider $V_c = 0$ and $L = 2$ kpc, values that fit the cosmic-ray (proton) radial distribution obtained from the gamma-ray emissivity. The relative spectra of the primary components obtained from our model for identical input spectra $\gamma_s = 2.2$ for all nuclei and for $K(P) \sim P^{0.6}$ (equivalent to $\lambda_{esc} \sim P^{-0.6}$ which provides a good fit to cosmic-ray data in conventional leaky box propagation models) are shown in Figure 3. The calculated B/C and $(Z = 21–23)$/Fe ratios are shown in Figures 4 and 5. The normalization for K required for these calculations is taken to be 6×10^{27} cm^2 s^{-1} at 1 GV. This choice will be justified in later calculations. Note that the primary spectra all show a progressively increasing turnover at low rigidities with increasing charge even without the effects of ionization energy loss or of convection. This is also true of the B/C and $(Z = 21–23)$/Fe ratios which provide an excellent fit to the observations.

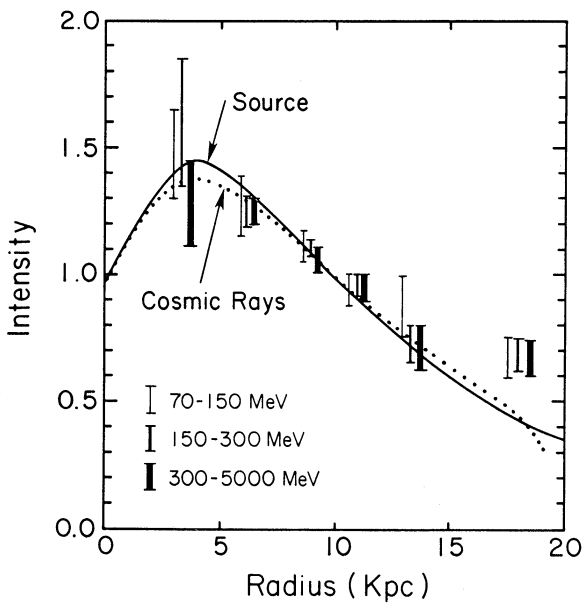

FIG. 2.—Cosmic-ray radial distribution for a modified source distribution, halo size $L = 2$ kpc. Cosmic-ray nuclei distribution from Bloemen (1989).

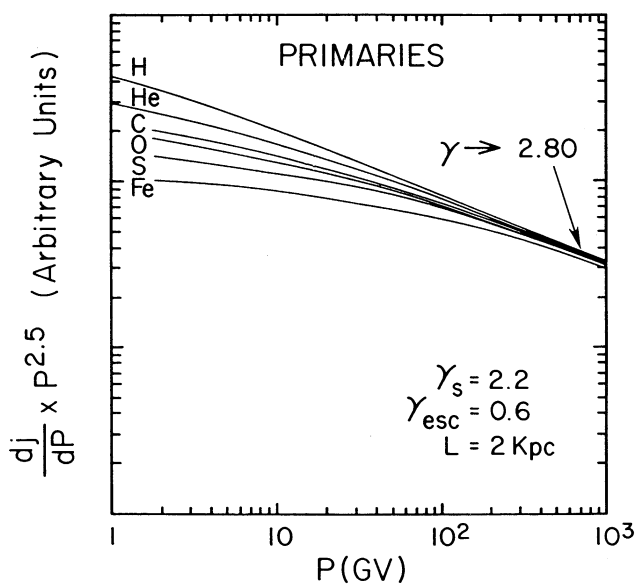

FIG. 3.—Spectra of primary components, normalized to the same source spectra, $\gamma_s = -2.2$ and with $K(P) \sim P^{0.6}$, $L = 2$ kpc and $V_c = 0$.

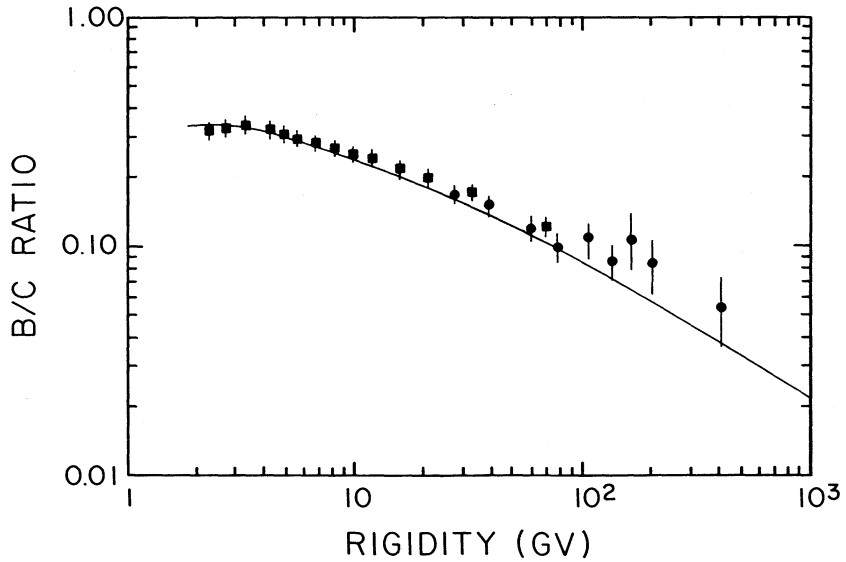

FIG. 4.—The B/C ratio as a function of energy. Same parameters as Fig. 3. Data from compilation by Gupta & Webber (1989).

Consider now specifically Be and the radioactive secondary ^{10}Be. At rigidities between 1 and 2 GV the measured Be/C ratio is 0.08 ± 0.01 and the fraction of ^{10}Be surviving, $f = 0.25 \pm 0.08$ (Mewaldt 1989). These two measurements are sufficient to define K and L as discussed below. In Figure 6 we show the Be/C ratio calculated from our model for various values of the ratio K/L. The B/C observations fix this ratio at $(8 \pm 1.6) \times 10^5$. In the LBM this is equivalent to determining the path length in g cm^{-2}. This ratio of K/L can be accomplished in several ways. If the thickness of the halo is made larger, then K must also be larger. In the calculation of Dogiel & Uryson (1988), for example, $K/L = 2.8 \times 10^6$ which would lead to a predicted Be/C ratio ~ 0.04, inconsistent with the measurements.

The ^{10}Be measurements, however, used in conjunction with the limits on K/L, set limits on the value of K, in fact the predicted ^{10}Be/Be ratio varies as $K^{0.5}$. To fit the ^{10}Be observations requires a value of $K \sim (6 \pm 4.0) \times 10^{27}$ cm^2 s^{-1}, thus fixing the value of $K(P)$ at 1 GV and the rigidity scale as noted previously. Taking this value of K in conjunction with the limits on K/L provided by the Be/C ratio leads to limits on $L = (2 + 1.8, -0.9)$ kpc. Thus an upper limit of $L < 4$ kpc is found for the halo thickness or equivalently $L/R < 0.2$, for the assumption that $V_c = 0$.

Now let us consider the case for $V_c > 0$ and the effects of varying the halo thickness from 1 to 16 kpc. This modifies all aspects of the calculations from the shape of the primary spectra to the secondary to primary ratios to the fraction of surviving radioactive secondaries depending on the values of V_c and L. We will illustrate some of these effects in what follows.

3.2.1. *Primary Spectra*

The effects of a changing V_c and L on the primary spectra are best illustrated by taking ratios of two primary species. The

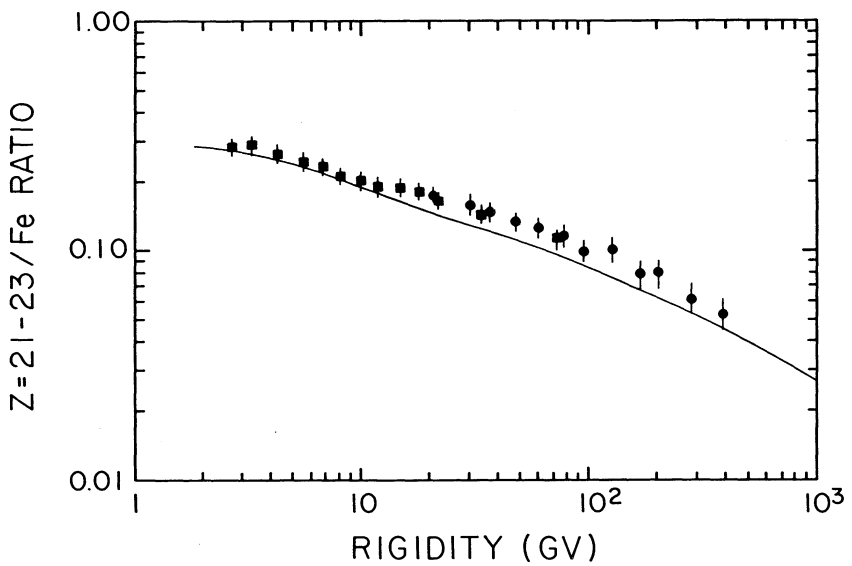

FIG. 5.—The (Z = 21–23)/Fe ratio as a function of energy. Same parameters as Fig. 3. Data from compilation by Grove et al. (1991).

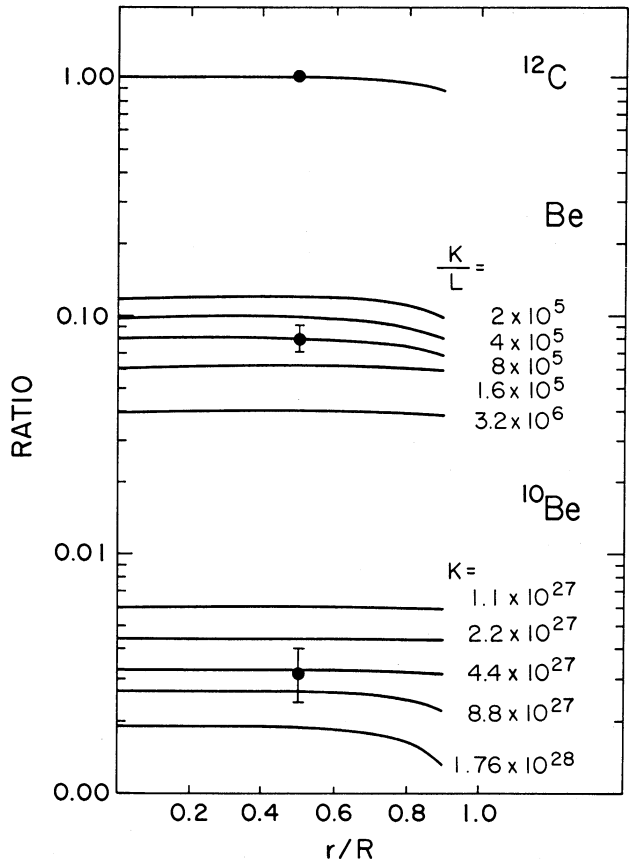

FIG. 6.—The Be/C and ^{10}Be/Be ratios at 1–2 GV. Data from Mewaldt (1989) and Wiedenbeck & Greiner (1980): predictions for $V_c = 0$.

He/O and O/Fe ratios calculated with K proportional to $P^{0.6}$ shown in Figures 7 and 8 illustrate the effects seen in all the primary to primary ratios. The low rigidity flattening of the primary spectra at increasingly higher rigidities for higher Z particles seen in Figure 3 arises because the particles interact in a thin matter disk and diffuse without interacting in a more extended halo. This interaction length is a strong function of charge and of energy so the resulting charge ratios, when plotted as a function of the lower Z to the higher Z element, also increase at low rigidities. For a given initial source abundance ratio the calculated ratio at low rigidities outside the heliosphere is therefore also a strong function of halo size for $V_c = 0$. Shown in these figures are the charge ratios calculated using the Saclay version of the LBM propagation program (see, e.g., Gupta & Webber 1989). This type of program has been used to calculate almost all source abundances reported in the literature and in these cases effectively corresponds to our diffusion model with a halo thickness ~ 4 kpc. By changing the source ratios other halo thicknesses could not be ruled out by the cosmic-ray data—so these primary ratios are not a sensitive test of halo size.

For $V_c > 0$ we show only one example, 80 km s^{-1}; smaller values of V_c will approach the $V_c = 0$ curves. The introduction of a finite convection velocity greatly modifies the primary-to-primary ratios particularly at low energies in essence because, for large convection velocities, all particles are quickly convected out of the system regardless of halo size L, so that only values of $V_c < 10$–20 km s^{-1} are consistent with the cosmic-ray data.

3.2.2. *Secondary-to-Primary Ratios*

Here we show in Figures 9 and 10 the B/C and ($Z = 21$–23)/Fe ratios calculated for various halo sizes with K as a function of rigidity and for $V_c = 80$ km s^{-1}. The curves for $L = 2$ kpc and $V_c = 0$ are identical to those in Figures 4 and 5. Here again the halo size makes an important difference in the calculated ratios, for the same reasons as discussed for the primary-to-primary ratios in the previous section; however, unlike the primary-to-primary ratios, these secondary ratios cannot be adjusted by the source composition but depend only on secondary production. Both of these secondary-to-primary ratios are therefore very sensitive indicators of the halo size and are only consistent with values of L between 2 and 4 kpc for $V_c = 0$.

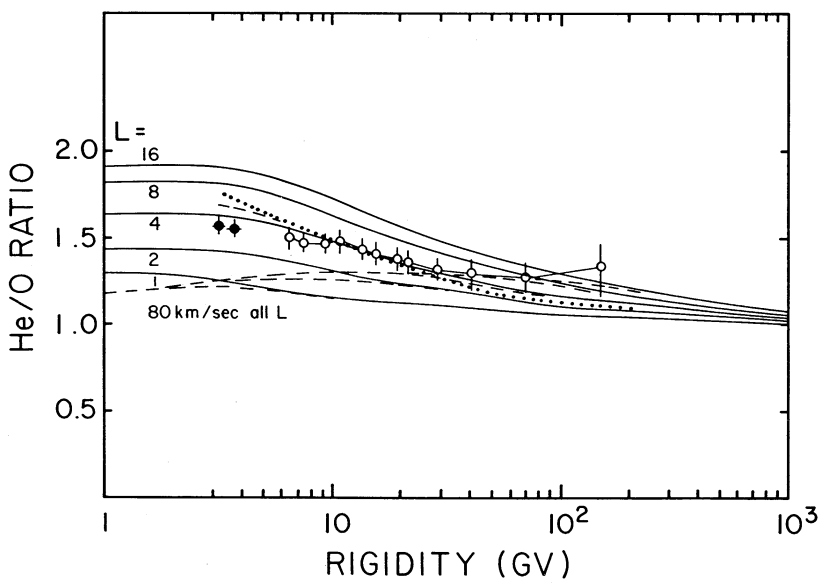

FIG. 7.—The calculated He/O ratio as a function of rigidity for various halo thicknesses in kpc (*solid lines*) and for $V_c = 80$ km s^{-1} (*dashed lines*). Abundance ratio at source = 26.6. Heavy dotted line is from an LBM calculation with the same escape length and cross section parameters. Data are from Engelmann et al. (1990) and Webber & Golden (1987).

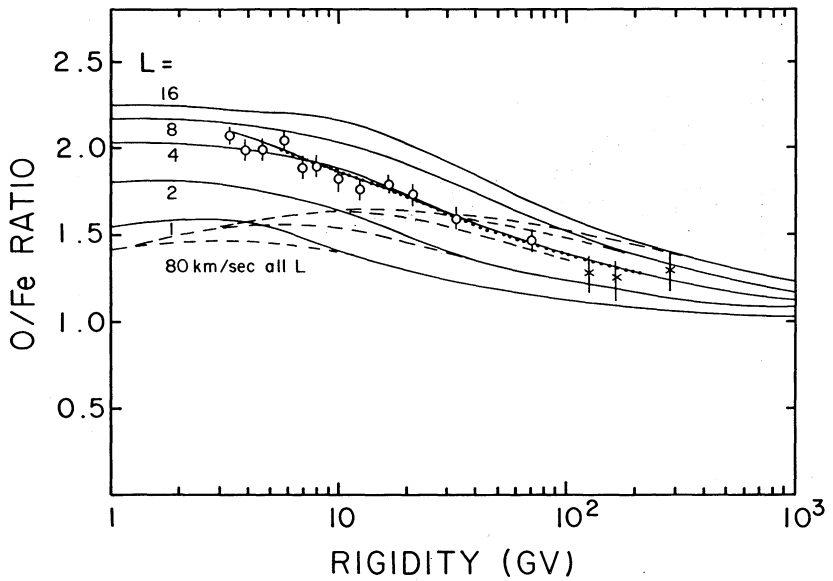

FIG. 8.—The calculated O/Fe ratio as a function of rigidity for various halo thicknesses in kpc (*solid lines*) and for $V_c = 80$ km s^{-1} (*dashed lines*). Heavy dotted line is from LBM calculation similiar to that in Fig. 7. Data are from Engelmann et al. (1990) and Swordy et al. (1990).

Here the introduction of a finite convection velocity again greatly modifies the secondary-to-primary ratios. Only values of $V_c < 10$–20 km s^{-1} are consistent with the cosmic-ray data. The interplay between L and V_c may be seen by looking at a fixed energy, 1 GeV per nucleon, where both the B/C and $Z = 21$–23/Fe ratios are well measured. This is illustrated in Figure 11 where the effect of both the halo size and convection velocity on these ratios is shown. The experimental data at 1 GeV per nucleon limits L to less than 3 kpc and V_c to less than 30 km s^{-1}. If the halo is very small, larger convection velocities are possible; conversely, if the halo is near its upper limit of 3 kpc, only small convection velocities are possible. This comparison at a fixed energy shows that the limitations on L and V_C implied by Figures 7–10 which examine the full rigidity-dependence are not simply a result of our choice of primary spectra or the dependence of the diffusion coefficient on rigidity.

3.3. *Radioactive Secondaries*

In Figures 12 and 13 we show the surviving fraction of ^{10}Be and ^{26}Al as a function of energy for different halo sizes and for $V_c = 80$ km s^{-1}. The curves for $V_c = 0$ are consistent with our earlier arguments that the ^{10}Be data indicate a halo size of $(2.0 + 1.8, -0.9)$ kpc. For ^{26}Al the limits on halo size are $(2.4 + 14.0, -1.6)$ kpc; because the ^{26}Al abundance is less well known it does not set an effective upper limit on the size of the halo. For $V_c > 0$ it is seen that the calculated value of the surviving fraction, f, at low energies for both ^{10}Be and ^{26}Al is a sensitive function of V_c. In effect these radioactive secondaries set the severest limits on V_c, while setting weaker limits on L.

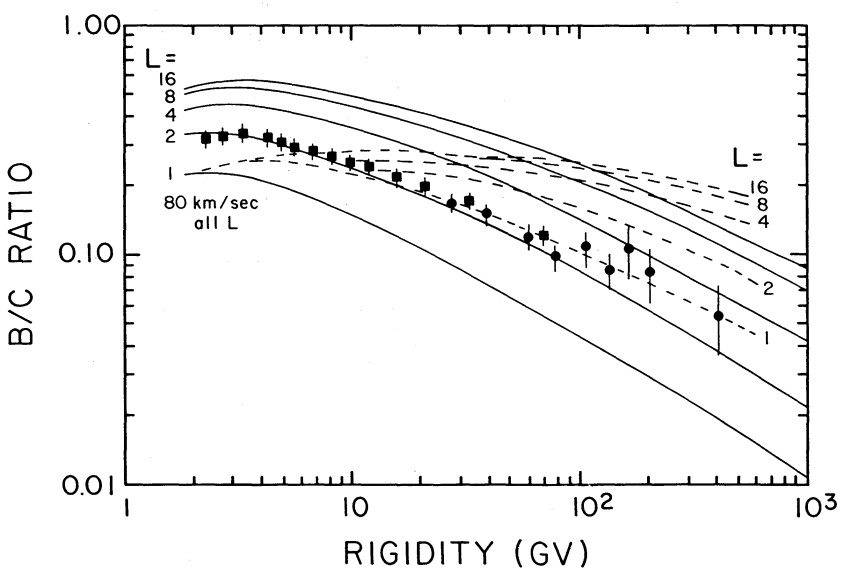

FIG. 9.—The calculated B/C ratio as a function of rigidity for various halo thicknesses in kpc and $V_c = 0$ (*solid lines*) and for $V_c = 80$ km s^{-1} (*dashed lines*). Data are from a compilation by Gupta & Webber (1989).

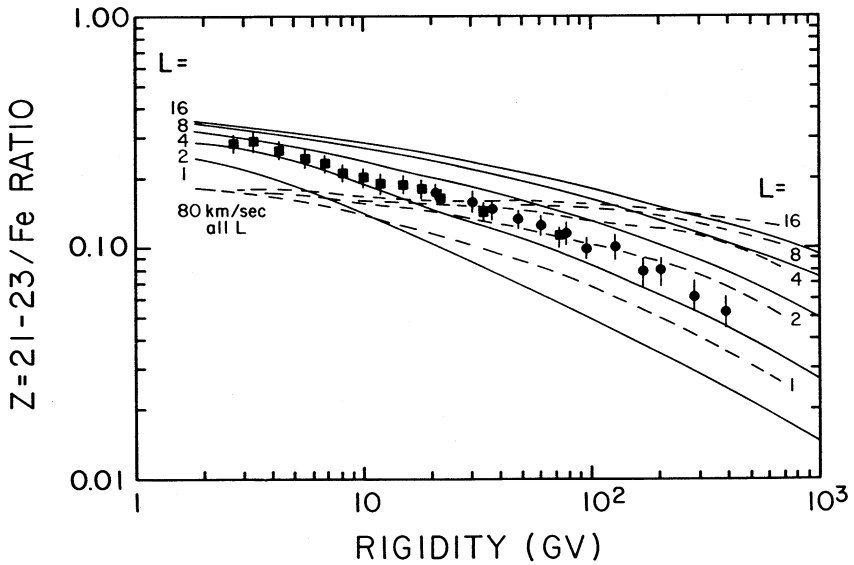

FIG. 10.—The calculated ($Z = 21$–23)/Fe ratio as a function of rigidity for various halo thicknesses in kpc and $V_c = 0$ (*solid lines*) and for $V_c = 80$ km s^{-1} (*dashed lines*). Data are from a compilation by Grove et al. (1991).

These conclusions are in agreement with those of Prishchep & Ptuskin (1975) and Freedman et al. (1980), based on diffusion models but using less recent data on Be and ^{10}Be in cosmic rays. These new limits are shown for ^{10}Be in Figure 14, where the data allow almost any halo size, but limits V_c to less than 30 km s^{-1}. Similar limits on V_c and L come from ^{26}Al. Improved measurements of ^{10}Be and ^{26}Al including measurements at more than one energy, used in conjunction with the limits on L set by the secondary-to-primary ratios, could further restrict the values of a galactic wind that are allowed by the cosmic-ray data.

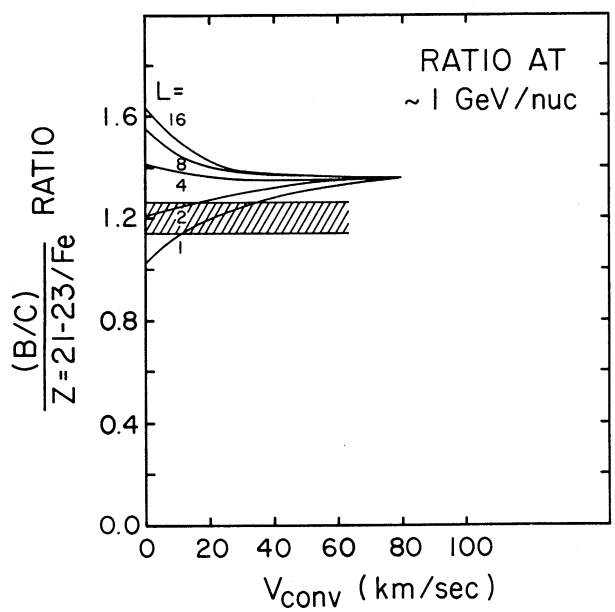

FIG. 11.—The ratio (B/C)/($Z = 21$–23)/Fe at a fixed energy of 1 GeV per nucleon as a function of halo thickness in kpc and convection velocity, V_c. Limits are from Engelmann et al. (1990).

4. SUMMARY AND CONCLUSIONS

We have developed a diffusion model for cosmic-ray propagation in the galaxy that includes the effects of convection in the halo. This model has several new features. The matter is assumed to be distributed within an infinitely thin disk within which the sources are also found. This permits a rather straightforward calculation of the radial cosmic-ray distribution as well as the effects of halo size and convection velocity on the cosmic-ray energy spectra and composition starting from various assumed source distributions. Another feature of our model is that detailed calculations of interaction loss rates, secondary production rates, and radioactive decay, all based on recent cross section measurements, are carried out for 13 separate cosmic-ray nuclei for rigidities between 1 and 10^3 GV in order to study the variations in primary spectra, secondary-to-primary ratios, and radioactive decay with an accuracy comparable to detailed LBM calculations.

The results of these calculations can be summarized as follows. (1) For the cosmic-ray radial distribution, in order to fit the rather weak radial dependence derived from gamma-ray data by Bloemen (1989), it is also necessary to have a rather flat radial distribution of cosmic-ray sources. This cosmic-ray radial distribution depends only weakly on the size of the halo; using an earlier steeper radial distribution of cosmic-ray sources presented by Stecker & Jones (1977), the predicted cosmic-ray radial profiles can only be made to fit (rather poorly) the radial profiles derived by Bloemen by using very large halos where $L/R > 0.75$. Flatter radial profiles for the cosmic-ray sources, consistent with what is now known about the radial distribution of pulsars and supernova remnants, fit the gamma-ray data rather well, implying that this class of sources may be considered viable candidates for the origin of cosmic rays. (2) The study of the primary-to-primary and secondary-to-primary cosmic-ray ratios as a function of rigidity along with the data on radioactive decay isotopes, when examined collectively, set quite stringent limits on both the halo thickness and the magnitude of a galactic wind. The primary-to-primary ratio variations as a function of rigidity (in

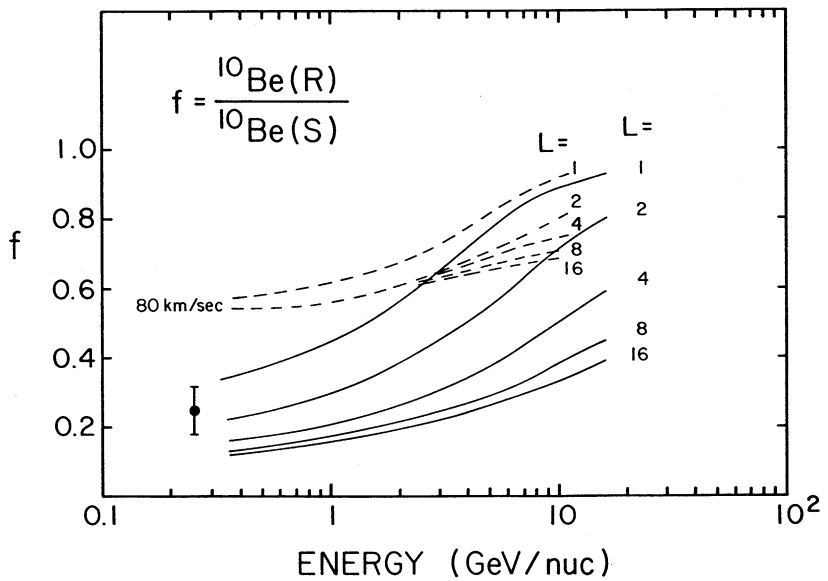

FIG. 12.—Surviving fraction of ^{10}Be as a function of energy calculated for various halo sizes (*solid lines*) and for $V_c = 80$ km s^{-1} (*dashed lines*). Data point is average of available data as discussed by Mewaldt (1989).

essence the rigidity spectra of these components) do not really restrict the halo size, if the source abundance is allowed to vary, but do restrict convection velocities to less than 20 km s^{-1}. The secondary-to-primary ratio variations as well as their absolute magnitude restrict both L and V_c. In general L must be less than 3 kpc and $V_c < 30$ km s^{-1}. Smaller halos lead to more stringent limits on V_c and vice versa. The surviving fractions of the radioactive secondaries, which are measured with limited accuracy at only one energy, restrict L/R to be <0.25 and limit V_c to <30 km s^{-1}, even with the large errors in the current data.

Overall the cosmic-ray data discussed here conservatively limit the cosmic-ray halo to a maximum thickness of 4 kpc and a convective galactic wind to less than 20 km s^{-1}, within a few kpc of the disk within the framework of our propagation model. These limits apply most strongly to rigidities of a few GV. The limits are interrelated, however, especially those derived from the secondary-to-primary ratios; e.g., if L approaches 4 kpc the V_c must be less than 10 km s^{-1} but if $L = 1$ kpc then V_c can be at most 35 km s^{-1}.

In examining the effects of a convective halo the quantity $q = V_c L/K$ is frequently defined. If $q > 1$ the cosmic-ray motion is said to be convection-dominated; if $q < 1$ it is diffusion-dominated. For a rigidity of 1 GV we find $K = 6 \times 10^{27}$ cm^2 s. If we take $L = 2$ kpc and $V_c < 10$ km s^{-1} from the secondary-to-primary ratios, then $q < 0.80$ with an upper limit, considering errors, of about 1.5. This suggests that below a few GV cosmic-ray propagation perpendicular to the disk is probably not convection-dominated—at best a combination of a weak convection velocity and a small K and L

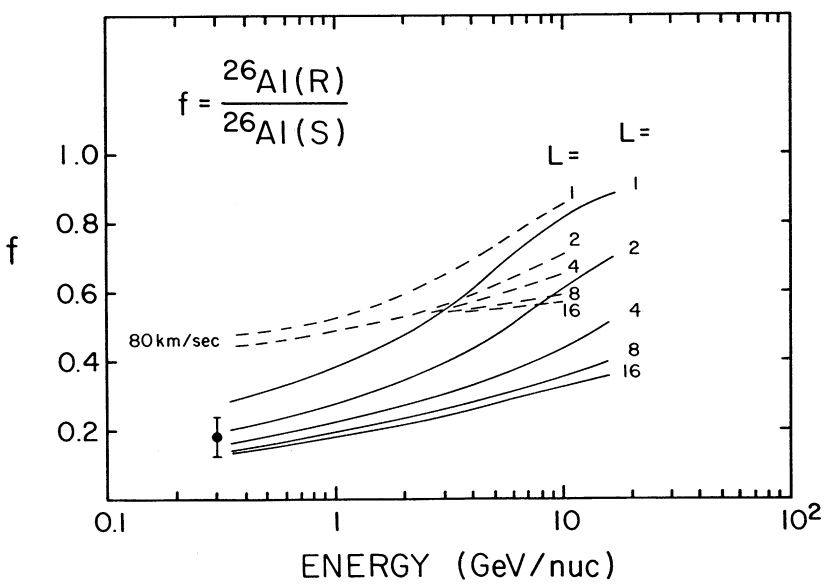

FIG. 13.—Same as Fig. 12 except for the surviving fraction of ^{26}Al.

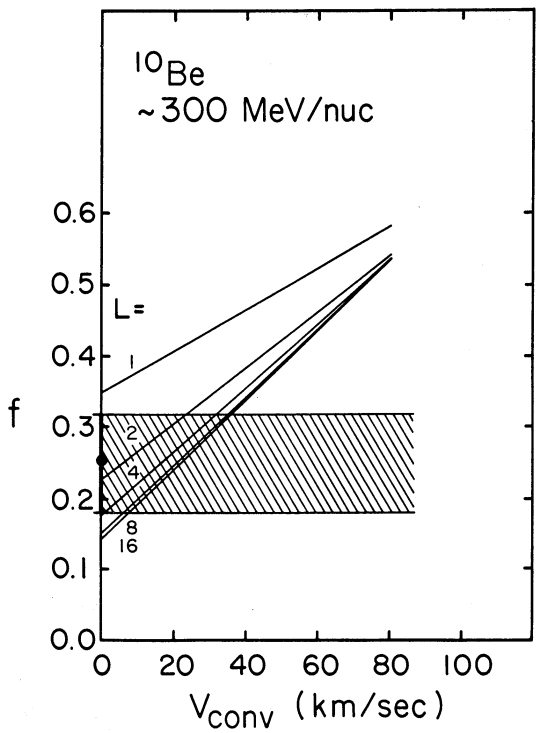

FIG. 14.—Surviving fraction of ^{10}Be at ~300 MeV per nucleon calculated as a function of halo size and convection velocity (scale fixed by the Be/C ratio). Data point is same as Fig. 12.

apply. Above, at few GV rigidity, diffusion clearly dominates since K becomes larger. This picture is consistent with the suggestion by Jones (1979) that convection is responsible for the low-energy flattening of the relationship between the escape length λ_{esc} and P. However, our analysis really only puts upper limits on the quantities L and V_c that enter into q. Modest improvements in the data, particularly for the radioactive secondaries, would allow these limits to be further refined. Our analysis further shows that a flattening of the B/C and (Z = 21–23)/Fe ratios at low rigidities occurs naturally in a diffusion model without the need for a convective term. This flattening arises because particles interact in a thin matter disk and diffuse without interacting in a more extended halo; this interaction length is a function of the decreasing particle velocity at low energies and also the changing cross sections with energy as we have noted earlier.

We are in the process of calculating corresponding distributions for electrons using a similar model but including the effects of energy loss. In this case the comparison can be made with the well-known distribution of radio synchrotron emission from the galaxy (e.g., Beuermann, Kanbach, & Berkhujsen 1985). With regard to the thickness of the radio halo, Beuermann et al. have noted that the half-power thickness for our galaxy is about 3.6 kpc. This value is consistent with measurements of other galaxies as well which find that the ratio L/R is typically between 0.2 and 0.4 (e.g., Hummel, Smith, & Van de Hulst 1984). These values would also be consistent with the halo thickness limits derived on the basis of cosmic-ray nuclei data in this paper.

This work was partially supported by NASA grants NAGW-1530 at the University of New Hampshire and NAGW-2016 at New Mexico State University (W. R. W.) and NSF grant ATM-8903703 and NASA grant NAGW-76 at the University of New Hampshire. (M. A. L.)

REFERENCES

Beuermann, K., Kanbach, G., & Berkhujsen, E. M. 1985, A&A, 153, 17
Bloemen, J. B. G. M. 1989, ARA&A, 27, 469
Bloemen, J. B. G. M., & Dogiel, V. A. 1992 A&A, in preparation
Dogiel, V. A., & Uryson, A. V. 1988, A&A, 197, 335
Engelmann, J. J., et al. 1990, A&A, 233, 96
Freedman, I., Giler, M., Kearsey, S., & Osborne, J. L. 1980, A&A, 82, 110
Ginsburg, V. L., Khazan. Y. A., & Ptuskin, V. S. 1980, Ap&SS, 68, 295
Grove, J. E., Hayes, B. T., Mewaldt, R. A., & Webber, W. R. 1991, ApJ, 377, 680
Gupta, M., Lee, M. A., & Webber, W. R. 1990, Proc. 21 Internat. Cosmic-Ray Conf., 3, 341
Gupta, M., & Webber, W. R. 1989, ApJ, 346, 1124
Hummel, E., Smith, P., & Van de Hulst, J. M. 1984, A&A, 137, 138
Jones, F. C. 1979, ApJ, 229, 747
Kassim, N. E. 1989, ApJ, 347, 915
Kota, J., & Owens, A. J. 1980, ApJ, 237, 814
Lerche, I., & Schlickeiser, R. 1982, MNRAS, 201, 1041
Lyne, A. G., Manchester, R. N., & Taylor, J. H. 1985, MNRAS, 213, 613
Mewaldt, R. A. 1989, AIP Conf. Proc. 183, Cosmic Abundances of Matter, ed. C. J. Waddington (New York: AIP) 124
Owens, A. J., & Jokipii, J. R. 1977, ApJ, 215, 677
Prishcep, V. L., & Ptuskin, V. S. 1975, Ap&SS, 32, 265
Soutoul, A., Engelmann, J. J., Ferrando, P., Koch-Miramond, L., Masse, P., & Webber, W. R. 1985, Proc. 19 Internat. Cosmic-Ray Conf., 2, 8
Stecker, F. W., & Jones, F. C. 1977, ApJ, 217, 843
Swordy, S. P., Muller, D., Meyer, P., L'Heureux, J., & Grunsfeld, J. M. 1990, ApJ, 349, 625
Webber, W. R., & Golden, R. L. 1987, Proc. 20 Internat. Cosmic-Ray Conf. 1, 325
Webber, W. R., Kish, J. C., & Schrier, D. A. 1990a, Phys. Rev. C, 41, 533
———. 1990b, Phys. Rev. C, 41, 547
———. 1990c, Phys. Rev. C, 41, 566
Wiedenbeck, M. E., & Greiner, D. E. 1980, ApJ, 239, L139